Preparation and Characterization of Nylon610/Functionalized Multiwalled Carbon Nanotubes Composites

Zhongyuan Li,[1,2] Shuzhen Xu,[1] Wentao Liu,[1] Suqin He,[1] Chengshen Zhu[1]

[1]*School of Materials Science and Engineering, Zhengzhou University, Zhengzhou, Henan 450052, China*
[2]*Quality and Technical Supervision Inspecting and Testing Center, Zhoukou, Henan 466000, China*

ABSTRACT: Nylon610 nanocomposites containing functionalized multiwalled carbon nanotubes (MWCNTs) were prepared using wet melt blending method, which is a novel preparation technique. In comparison with the pure nylon610, the elastic modulus, tensile strength, bending modulus, and bending strength of the composites increase significantly with the increase of MWCNTs content, and the mechanical properties of the composites are also improved significantly by adding a small amount of MWCNTs (0.1 wt %). The crystallization peak of the composites shifts to higher temperature with the addition of MWCNTs, and among the two melting peaks, the intensity of melting peak at low temperature decreases with increasing MWCNTs content. The composites are more stable than pure PA610 and decompose at higher temperature, suggesting that the accession of MWCNTs can improve the composites' thermal stability. The storage modulus of the composites decreases with the temperature increasing, but under lower temperature it increases significantly with the addition of MWCNTs–COOH except for PANT-0.1 sample. Transmission electron microscope (TEM) images of composites exhibit that the wet melt blending technique can avoid the excess agglomeration of MWCNTs under vacuum dryness, which benefits MWCNTs to disperse uniformly in matrix. © 2009 Wiley Periodicals, Inc. J Appl Polym Sci 113: 2805–2812, 2009

Key words: irradiation; nylon; melt; blending; composites

INTRODUCTION

Since the discovery of carbon nanotubes (CNTs) by Iijima in 1991, CNTs have attracted tremendous attention of many researchers due to their unique properties such as higher aspect ratio, higher mechanical strength, and higher electrical and thermal conductivity.[1,2] One of the most promising applications of CNTs is polymer/CNTs nanocomposites.[3] The combination of their outstanding physical properties often makes CNTs as an excellent reinforcing material for high-performed and multifunctional polymeric nanocomposites.[4,5] Polymer/CNTs nanocomposites, including the polyethylene,[6,7] and polypropylene,[8,9] polycarbonate,[10,11] polystyrene,[12] and polyamide[13–15] matrices have been studied. However, it is difficult to achieve homogenous dispersion of CNTs within polymer matrices, because of the extremely surface energy of CNTs and high interbundle Van Der Waals interactions between carbon nanotubes. This dramatically hinders rapid progress in the application field of CNTs. Meanwhile, it is difficult to achieve strong interfacial adhesion between carbon nanotubes and matrix. To overcome these technical hurdles, it is desirable to modify the CNTs surface to enhance the compatibility with polymer matrix. Chemical and physical methods have been used to modify the CNTs,[16,17] and the more effective is the chemical methods.

Polyamide (Nylon) is the head of the five engineering plastics with numerous applications. Recently, nylon/CNTs nanocomposites have been investigated by many research groups, and many methods have been applied, such as the physical mixing of the carbon nanotubes with nylon in solution or in molten state, melt spinning, *in situ* polymerization in the presence of carbon nanotubes.[18–28] Consequently, impressive progress has been achieved. For example, Chen et al.[18] prepared multiwalled carbon nanotubes (MWCNTs) reinforced nylon 6 composites by the simple melt compounding approach. The Young's modulus and tensile strength of nylon 6 were greatly improved by the incorporation of MWCNT, and further microscopic observations revealed that a more uniform and fine dispersion of MWCNT was achieved throughout the nylon 6 matrix because of the stronger interfacial

adhesion between the nanotubes and the matrix. Sandler, et al.[27] prepared polyamide-12 fibers reinforced with carbon nanotubes and nanofibers by melt spinning, and the vapor-grown carbon nanofibers and CVD-grown MWCNTs dispersed well into the matrix and provided linear increase in initial stiffness and yield strength for composites as a function of loading fraction. Kang, et al.[20] prepared nylon610/carbon nanotube composite by *in situ* interfacial polymerization. The tensile tests of the composite sheet showed that the Young's modulus increases by 170% and the tensile strength and the elongation at break slightly increase by 40 and 25%, respectively. Furthermore, scanning electron microscope photograph disclosed that the individual MWCNTs were uniformly dispersed in the nylon610 matrix.

In this study, we present a new functionalizing MWCNTs method, namely, radiating MWCNTs in a mixture of sulfuric and nitric acids. The carboxyl groups were grafted to the surface and side wall of MWCNTs. The composites were prepared via a wet melt blending process. This wet melt blending method, which can improve commercial application of PA610/MWCNTs composites, is simple and easier for preparation of PA610/MWCNTs compared with *in situ* polymerization. The structure of functionalized MWCNTs was characterized and the mechanical properties, melting and crystallization properties, microstructure, thermal degradation behavior, and the thermomechanical properties of the resulting composites were explored.

EXPERIMENTAL

Materials

Nylon610 powder (PA610) was purchased from Shanghai Zhenwei Composites (China) with a viscosity average molecular weight being 13,000. The MWCNTs were purchased from Shenzhen Nanaotech Port (China) with length ranging from 5 to 15 μm and purity ranging from 95 to 98%.

Modification of MWCNTs

To remove the impurities (such as the metallic catalysts particles, amorphous carbon, and so on) in the MWCNTs powder and make the MWCNTs be grafted with carboxyl groups, MWCNTs were radiated in nitric and sulfuric acids (analytical purity, volume ratio (1 : 3)) via $^{60}C_O$ gamma X-ray with 200 kGy irradiation dose for 8 h at room temperature. The mixture was vacuum-filtered through a 0.45-μm poly(vinylidene fluoride). Millipore membrane, and washed with distilled water until the pH value of the filtrate was ca. 7. A little filtered solid was dried under vacuum at 60°C for 24 h and the water weight fraction of wet MWCNTs was measured. The modified MWCNTs were marked as MWCNTs–COOH.

Preparation of PA610/MWCNTs–COOH composites

According to the water weight fraction of wet MWCNTs–COOH and the MWCNTs–COOH weight fraction in composites, a determinate wet MWCNTs–COOH and silane coupling agent KH570 (1 wt % water solution) with a weight ratio of 0.5 : 100 were weighed and dispersed in distilled water under ultrasonication at 40°C for 1 h. Then the resulting suspending solution was mixed with PA610 powder using high-speed mixer and the final mixture was dried under vacuum at 90°C for 24 h. The PA610/MWCNTs–COOH composites containing 0.1, 0.5, 1.0, and 2.00 wt % of MWCNTs–COOH (marked as PANT-0.1, PANT-0.5, PANT-1.0, and PANT-2.0), were prepared via melt blending process using a TE-34 type twin-screw extruder. The temperature of the extruder was maintained at 195, 240, 250, 250, and 235°C from hopper to die, respectively. The rotation speed of the twin-screw was 30 rpm. The neat PA610 was also extruded through the same process. All the samples were dried under vacuum at 90°C for 24 h to remove any remaining water before injection molding. The test specimens of bar and dumbbell shape were injection molded using a HTF90-W2 type injection molder.

Characterization

A Nicolet 460 type Fourier transform infrared (FTIR) spectrometer was used to investigate the structure of pristine MWCNTs (p-MWCNT) and MWCNTs–COOH.

The mechanical properties were measured on CMT 5104 type universal test equipment at room temperature. The rate of extension and bending were 20 and 2 mm/min, respectively.

Dynamic mechanical analysis (DMA) was performed with the sample size of $54.0 \times 10.0 \times 4.0$ mm^3 on a NETZSCH-DMA 242 C type dynamic mechanical analyzer in a temperature range from room temperature to 210°C at a frequency of 1 Hz.

The melting and crystallization behaviors and thermal degradation behavior were studied using NETZSCH-STA 449 C type DSC/TG test equipment under nitrogen atmosphere at a heating rate of 10 and 20°C/ min, respectively.

The dispersion of MWCNTs in the PA610/ MWCNTs composites was investigated on a transmission electron microscope (TEM, Tecnai G2 20 S-twin, FEI. Co. Holand) at an accelerate voltage of 200 kv.
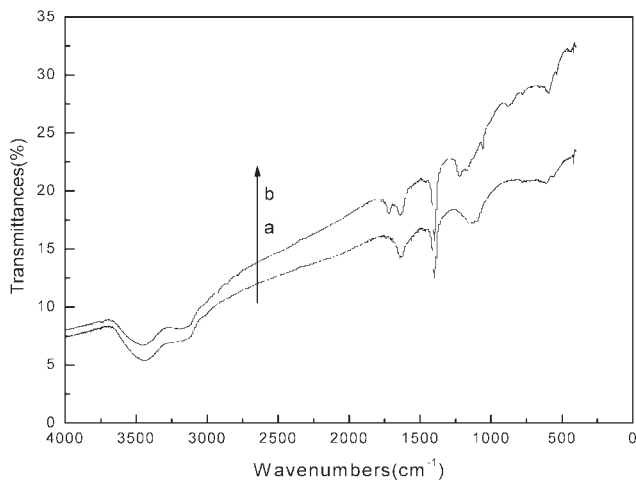
Figure 1 FTIR spectra of p-MWCNT (a) and MWCNT–COOH (b).
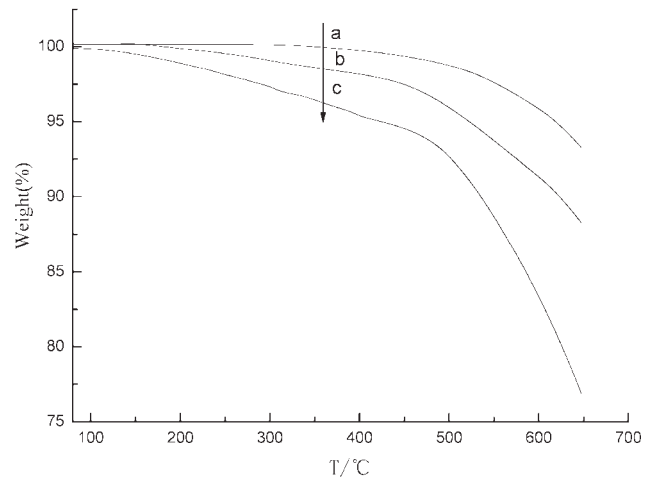
Figure 2 TG curves of crude MWCNTs and functionalized MWCNTs: Crude MWCNTs (a), MWCNTs functionalized without irradiation (b), and MWCNTs functionalized after irradiation (c).
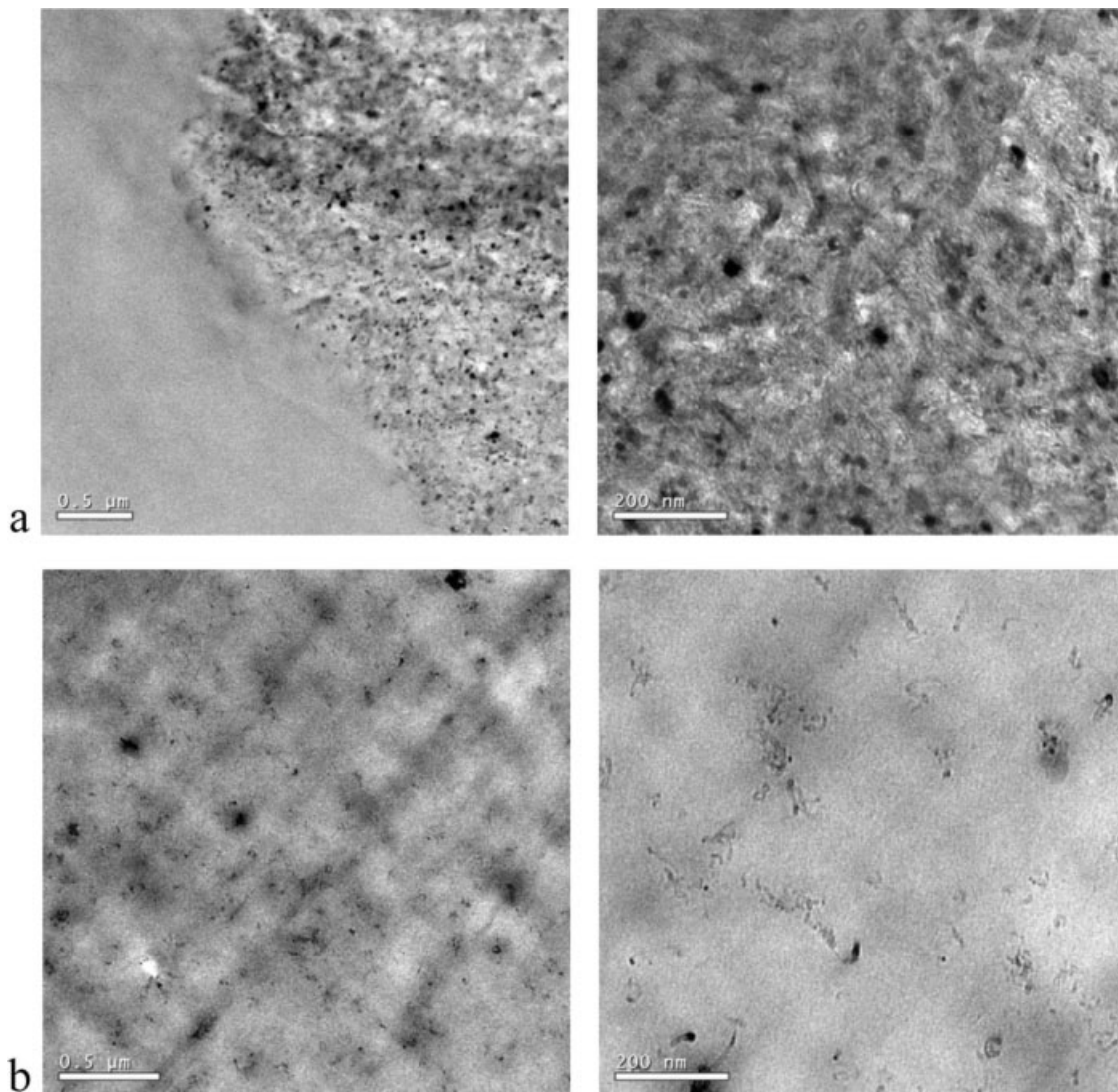
Figure 3 TEM photographs of the PA610/MWCNTs composites: melt compounding methods (a), wet melt blending methods (b).

TABLE I
Mechanical Properties of PA610 and PA610/MWCNT Composites

Sample	Elastic modulus (GPa)	Tensile strength (MPa)	Elongation at break (%)	Bending modulus (GPa)	Bending strength (MPa)	Impact strength (kJ/m^2)
PA610	1.64	46.51	275.7	1.37	39.01	4.49
PANT-0.1	1.75	53.30	230.5	1.57	44.69	4.20
PANT-0.5	1.88	54.31	92.44	1.61	45.73	3.19
PANT-1.0	1.91	52.48	4.39	1.66	46.38	2.85
PANT-2.0	2.04	51.60	5.59	1.77	46.89	2.58

RESULTS AND DISCUSSION

Characterization of MWCNTs

Figure 1 shows the FTIR spectra of p-MWCNTs and MWCNTs–COOH. Evidently, two wide peaks appear at 3200–3500 cm^{-1} regions, which can be attributed to the stretching vibration of hydroxyl group. A new peak appearing at 1720 cm^{-1} for MWCNTs–COOH may represent the stretching vibration of carbonyl group, indicating that carboxyl groups have been successfully grafted to MWCNTs.

As shown in Figure 2, the crude MWCNTs has a weight loss of about 5% at 635°C. However, a weight loss of 5% for the functionalized MWCNTs without irradiation (MWCNTsT) and under irradiation (MWCNTsTI) occurs at 522 and 424°C, respectively. Similar to that of crude MWCNTs, the TG analysis curves of the functionalized MWCNTs also show a sharp weight loss with increasing temperature before 635°C and that for MWCNTsTI exhibits more sharp loss than MWCNTsT. These results indicate that irradiation can cut the MWCNTs and increase the active spots at the side wall and end of MWCNTs, which leads to more graft of carboxyl and hydroxyl groups compared with that without irradiation.

TEM investigation of the composites

As can be seen in Figure 3, the MWCNTs in PA610/MWCNTs composites prepared by melt compounding methods agglomerate severely, despite compounding with commercial PA610 in two screw extruder, which results in stress convergence. Approximately, the MWCNTs of the composites dried in vacuum oven agglomerate badly before compounding with commercial PA610, and thereby being difficult to disentangle for composites. Whereas the MWCNTs has better dispersion in PA610/MWCNTs composites prepared by wet melt blending methods compared with above materials.

Mechanical properties of the composites

The effect of MWCNTs–COOH on the properties for reinforced composite evaluated by measuring the mechanical properties can be seen in Table I. The elastic modulus, tensile strength, bending modulus, and bending strength for the pure nylon610 are 1.64 GPa, 46.51 MPa, 1.37 GPa, and 39.01 MPa, respectively. As added with MWCNTs, those parameters of the composites increase significantly, the elastic modulus, tensile strength, bending modulus, and
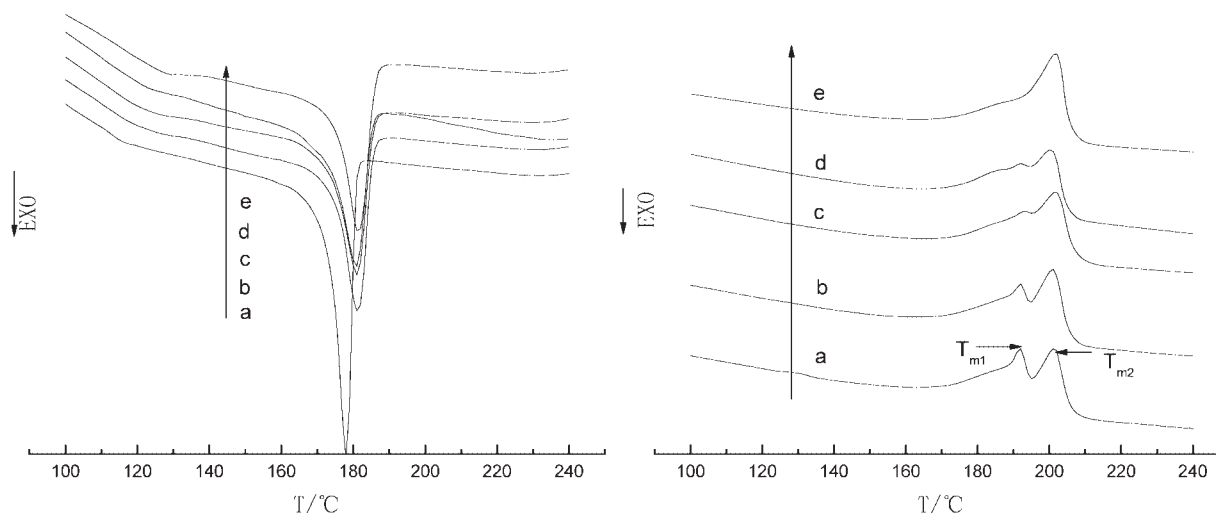
Figure 4 Nonisothermal DSC thermogram for pure PA610 and its composites: PA610 (a), PANT-0.1 (b), PANT-0.5 (c), PANT-1.0 (d), and PANT-2.0 (e).

TABLE II
Crystallization Parameters of PA610 and its Composites Measured by DSC

Sample	T_{ci} (°C)	T_c (°C)	$T_{cf}/$(°C)	ΔT_c (°C)	ΔH_c (J/g)	FWHM (°C)
PA610	180.8	178.0	173.3	7.5	−43.41	4.72
PANT-0.1	185.2	181.3	175.3	9.9	−33.44	7.28
PANT-0.5	185.4	181.0	174.4	11.0	−38.37	8.16
PANT-1.0	185.1	180.7	174.8	10.3	−30.33	7.52
PANT-2.0	186.1	181.5	175.6	10.5	−32.07	8.08

bending strength of the composites maximally increase by ca. 16.5, 16.8, 21.2, and 18.9%, respectively. However, the elongation at break and impact strength, which are indicator of a material's toughness, decrease dramatically with increasing MWCNTs content. From Table I, it can be concluded that the integrated mechanical properties of the composites increase significantly after adding a small amount of MWCNTs–COOH (0.1 wt %) into nylon610 powder, perhaps due to a homogeneous dispersion of MWCNTs–COOH in nylon610 matrix and strong interface adhesion between the functionalized MWCNTs–COOH and nylon610 matrix. The carboxyl and hydroxyl groups grafted on the end and side wall of MWCNTs improved the compatibility of PA610 with functionalized MWCNTs. However, the composites become brittle when MWCNTs–COOH content is too high owing to the nonhomogeneous dispersion of MWCNTs in nylon610 matrix, which stresses the concentration by MWCNTs' agglomeration.

## Melting and crystallization behaviors of the composites measured by DSC

Usually, the crystal form influences on the mechanical property of the composites. Therefore, to explore mechanism for the high mechanical strength of the composites, their melting and crystallization behaviors were investigated by DSC. Figure 4 shows the cooling and heating thermogram of PA610 and its composites obtained at a 10°C/min rate. The crystallization and melting parameters of PA610 and its composites are listed in Table II and Table III. T_{ci}, T_c, T_{cf}, ΔT_c, ΔH_c, and FWHM represent the initial crystallization temperature, crystallization temperature, final crystallization temperature, crystallization temperature range, crystalline enthalpy and half-height width, respectively, and the value of ΔT_c can be obtained according to the equation $\Delta T_c = T_{ci} - T_{cf}$. T_{mi}, T_m, T_{mf}, ΔH_m, ΔT_m, and C_m represent the initial melting temperature, peak melting temperature, final melting temperature, melting enthalpy, melting range, and crystallinity, respectively, and the value of ΔT_m and C_m can be obtained according to the equation $\Delta T_m = T_{mf} - T_{mi}$ and $C_m = \Delta H_m / \Delta H_m^0 \times 100\%$, respectively (Here, $H_m^0 = 200.83$ J/g[29]). The crystallization temperature (T_c) obtained from the exothermic peak is about 178.0°C for PA610. The crystallization peak of the composites shifts towards high temperature. Accordingly, T_c, T_{ci}, and T_{cf} increase with the addition of MWCNTs–COOH. It is because that the MWCNTs–COOH acting as nucleators interactions between the MWCNTs–COOH and PA610, which makes nylon molecular chains easily develop into crystals. Both ΔT_c and FWHM of composites are wider obviously than those of pure PA610, and increase by 2–4°C, indicating that the crystallization process slows down. However, the ΔH_c value of composites is basically lower than that of pure PA610, which can be explained by the addition of carbon nanotubes, which reduces the movement of molecular chains.

DSC heating curves in Figure 4 display two melting peaks at 192°C (T_{m1}) and 201°C (T_{m2}). The intensity of the lower temperature melting peak decreases after incorporating the MWCNTs with pure PA610. Double melting peaks are a universal phenomenon

TABLE III
Melting Parameters of PA610 and its Composites Measured by DSC

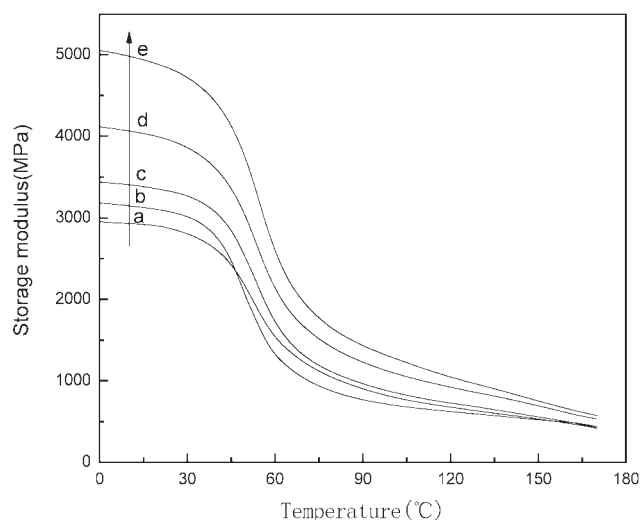| Sample	T_{mi} (°C)	T_m (°C)	$T_{mf}/$(°C)	ΔT_m (°C)	ΔH_m (J/g)	C_m (%)
PA610	188.7	191.7 201.1	205.7	17.0	43.61	21.7
PANT-0.1	193.2	192.1 201.1	205.7	12.5	45.21	22.5
PANT-0.5	196.9	192.3 201.6	207.1	10.2	45.97	22.9
PANT-1.0	197.7	192.0 200.1	205.2	7.5	47.35	23.6
PANT-2.0	193.4	201.6	206.0	12.6	48.47	24.1
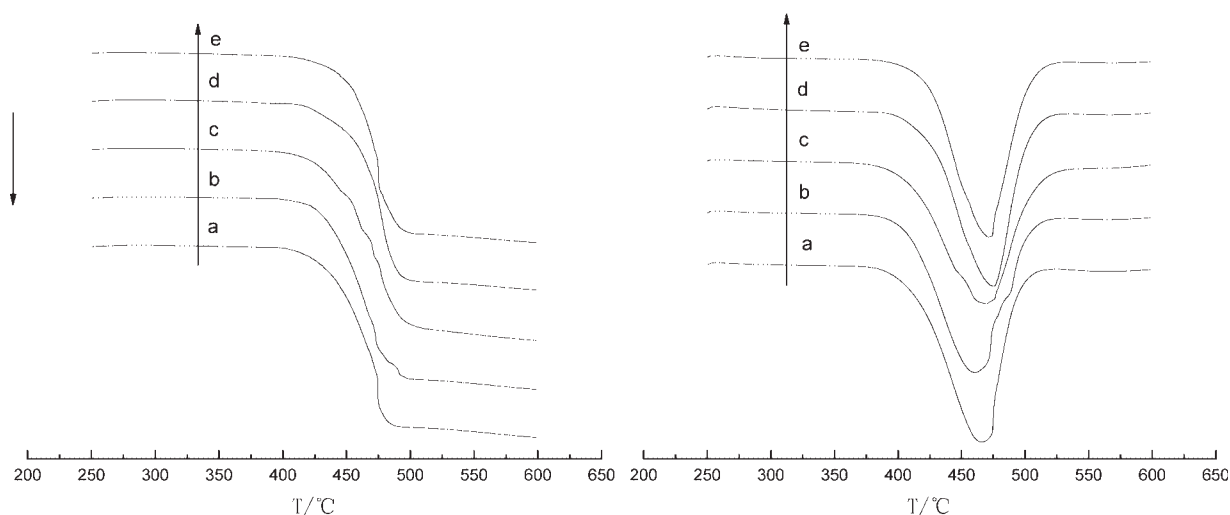
Figure 5 TG and DTG curves of pure PA610 and its composites: PANT-0.1 (a), PA610 (b), PANT-0.5 (c), PANT-2.0 (d), and PANT-1.0 (e).

that occurs during the melting process of pure PA610 and results from the PA610 melt recrystallization. It was reported that[20] the lower temperature melting peak corresponds to crystal melting of polymer, and the higher temperature melting peak corresponds to the melting of the recrystallized polymer. For the composites, the lower temperature melting peak intensity decreases, implying that recrystallized PA610 molecular chains manifold and crystal becomes more perfect. Moreover, C_m increases with the increment of MWCNTs content. At the same time, T_{mi} of composites is higher than that of pure PA610. However, T_{mf} changes a little. The melting range of composites becomes narrow after incorporating the MWCNTs into pure PA610. The value of ΔH_m of composites increases with the increase of MWCNTs content, and is clearly higher than that of pure PA610.

Thermogravimetric analysis of the composites

TG and DTG curves of PA610 and its composites were obtained by heating the samples up to 600°C at a rate of 20°C/ min under N_2 gas atmosphere (as shown in Fig. 5). The initial thermal decomposition temperature (T_{di}), the fastest decomposition temper-

ature (T_d), and final decomposition temperature (T_{df}) are listed in Table II. From Figure 5 and Table IV, it can be seen that the T_{di}, T_d, and T_{df} increase conclusively with increasing MWCNTs content. Compared with the pure PA610, the T_{di} of the composites increases by 3–13°C, T_d of the composites increases by 3–9°C, and T_{df} of the composites increases by 6–16°C. The PA610/MWCNTs–COOH composites decompose at higher temperature than pure PA610, suggesting that the accession of MWCNTs–COOH increases the thermal stability of the composites. It is well known that the enhanced thermal conductivity of a composite can facilitate heat transport and increase its thermal stability through the accession of high thermal conducting CNTs.[29,30] Our research results are in good agreement with that.

TABLE IV
Values of T_{di}, T_d, and T_{df} Measured by TGA for PA610 and its Composites

Sample	T_{di} (°C)	T_d (°C)	T_{df}/(°C)
PA610	384.4	466.1	514.6
PANT-0.1	387.9	460.0	520.3
PANT-0.5	376.0	468.7	530.5
PANT-1.0	396.6	474.8	522.9
PANT-2.0	390.1	471.7	520.6
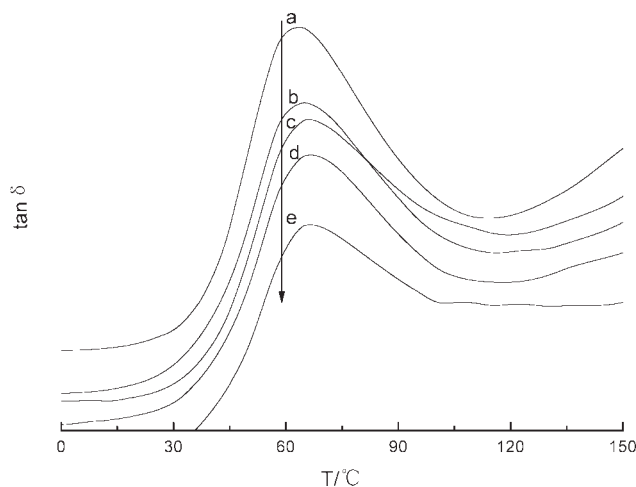
Figure 6 Curves of storage modulus vs temperature DMA for PA610 and its composites: PA610 (a), PANT-0.1 (b), PANT-0.5 (c), PANT-1.0 (d), and PANT-2.0 (e).
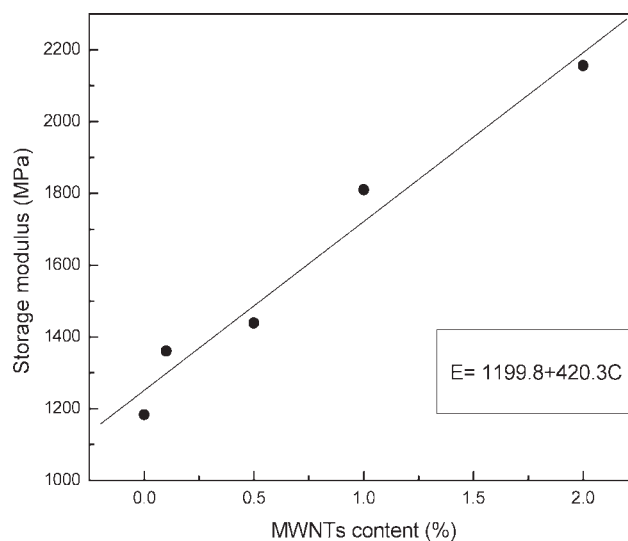
Figure 7 Curves of tanδ vs temperature DMA for PA610 and its composites: PA610 (a), PANT-0.1 (b), PANT-0.5 (c), PANT-1.0 (d), and PANT-2.0 (e).

Thermomechanical properties of the composites measured by DMA

Figure 6 shows the curves of the storage modulus vs temperature (DMA) for various PA610 composites with different MWCNTs–COOH content, and Figure 7 shows the tanδ value as a function of temperature for PA610 and PA610/MWCNTs–COOH composites. The glass transition temperature (T_g) being represented by the loss peak temperature can be deduced from Figure 7. Table V shows the T_g values of PA610 and its composites.

The storage modulus decreases with the temperature increasing, but it increases significantly with the addition of MWCNTs–COOH except for PANT-0.1 sample. From Table V, it can be seen that the T_g values of the composites being in a range from 65.0 to 66.5°C are higher than that of neat PA610 (the T_g values of neat PA610 being 63.7°C). It indicates that the interaction between MWCNTs–COOH and PA610 molecular chains restricts the movement of PA610 molecular chain segments. Figure 8 shows the curves of storage modulus vs MWCNTs content at T_g. It is evident that the storage modulus is linear dependence with MWCNTs content. The linear connection formula also given in Figure 8 shows $E = 1199.8 + 420.3C$ (here, E represents storage

TABLE V
T_g **Values of PA610 and its Composites Deduced by DMA**

Sample	T_g (°C)
PA610	63.7
PANT-0.1	65.0
PANT-0.5	66.2
PANT-1.0	66.5
PANT-2.0	66.4

Figure 8 Curves of storage modulus vs MWCNT content connection at T_g.

modulus and C represents MWCNTs content). The composite with 2.0 wt % MWCNTs–COOH addition displays the increment of storage modulus by about 88.2% (2156.1MPa) compared with PA610 (1183.1Mpa) at the glass transition temperature (T_g). It is obvious that the tanδ value for the composites is lower than that of the pure PA610 and decreases with adding MWCNTs–COOH content. As a result of MWCNTs–COOH addition, the loss peak transfers toward a higher temperature region when MWCNTs content further increases. To some extent, the covalent bonding and interconnection between PA610 and MWCNTs–COOH restrict the movement of the PA610 chain segments, which may result in the observed shift of the loss peak.

CONCLUSIONS

PA610/MWCNTs–COOH composites have been prepared by a novel wet melt blending technique and determined. The peak at 1720cm^{-1} in the FTIR spectra indicate that carboxyl groups have been grafted to MWCNTs. TG analysis of the functionalized MWCNTs indicate that irradiation can cut the MWCNTs and increase the active spots at the side wall and end of MWCNTs, which leads to more graft of carboxyl and hydroxyl groups compared with that without irradiation. Very interestingly, the elastic modulus, tensile strength, bending modulus, and bending strength for the composites are increased significantly with increasing MWCNTs content and maximally increased by ca. 16.5, 16.8, 21.2 and 18.9%, respectively. The compositive mechanical properties of the composites are increased significantly by addition of MWCNTs (0.1 wt %), and the composites become brittle when MWCNTs

content is too high. After incorporation MWCNTs with PA610, the crystallization peak of PA610/MWCNTs composites shifts toward high T_c and the initial crystallization temperature increases with the addition of MWCNTs–COOH. The crystallization peak of the composites is wider than that of PA610 and the ΔH_c value of composites is lower than that of pure PA610. Both pure PA610 and its composites show two melting peaks, and the intensity of melting peak at low temperature is decreased when MWCNTs content further increases. TGA analyses show that the composites decompose at higher temperature than pure PA610, suggesting that the accession of MWCNTs improves the thermal stability of the composites. DMA shows that the storage modulus of the materials enhances significantly with the addition of MWCNTs except for PANT-0.1 sample and that the tanδ value of the composites is lower than the pure PA610 and decreases with increasing MWCNTs content. Clearly, it is a simple and effective modified method to radiate MWCNTs in mixture of nitric and sulfuric mixed acids. TEM images of composites exhibit that the wet melt blending technique can avoid the excess agglomeration of MWCNTs under vacuum dryness, which benefits MWCNTs to disperse uniformly in matrix.

References

1. Baughman, R. H.; Zakhidov, A. A.; de Heer, W. A. Science 2002, 297, 787.
2. Iijima, S. Nature 1991, 354, 56.
3. Moniruzzaman, M.; Winey, K. I. Macromolecules 2006, 39, 5194.
4. Kodjie, S. L.; Li, L. Y.; Li, B.; Cai, W. W.; Li, C. Y.; Keating, M. J Macromol Sci B 2006, 45, 231.
5. Li, L. Y.; Li, C. Y.; Ni, C. Y.; Rong, L. X.; Hsiao, B. Polymer 2007, 48, 3452.
6. Zhang, Q. H.; Rastogi, S.; Chen, D. J.; Lippits, D.; Lemstra, P. J. Carbon 2006, 44, 778.
7. McNally, T.; Potschke, P.; Halley, P.; Murphy, M.; Martin, D.; Steven, E. J. B.; Brennan, G. P.; Bein, D.; Lemoine, P.; Quinn, J. P. Polymer 2005, 46, 8222.
8. Bhattacharyya, A. R.; Sreekumara, T. V.; Liu, T.; Kumar, S.; Ericsonb, L. M.; Haugeb, R. H.; Richard, E. S. Polymer 2003, 44, 2373.
9. Seo, M. K.; Lee, J. R.; Park, S. J. Mater Sci Eng A 2005, 404, 79.
10. Sung, Y. T.; Han, M. S.; Song, K. H.; Jung, J. W.; Lee, H. S.; Kum, C. K.; Joo, J.; Kim, W. N. Polymer 2006, 47, 4434.
11. Potschke, P.; Bhattacharyya, A. R.; Janke, A. Carbon 2004, 42, 965.
12. Watts, P. C. P.; Ponnampalam, D. R.; Hsu, W. K.; Barnes, A.; Chambers, B. Chem Phys Lett 2003, 378, 609.
13. Jia, Z. J.; Xu, C. L.; Liang, J.; Wei, B. Q.; Wu, D. H.; Zhu, S. W. N Carbon Mater 1999, 14, 32.
14. Jia, Z. J.; Wang, Z. Y.; Xu, C. L.; Liang, J.; Wei, B. Q.; Wu, D. H.; Zhang, Z. M. J Tsinghua Univ (Sci &Tech) 2000, 40, 14.
15. Yu, Y.; Liu, B.; Wang, W. J.; Zhang, P. China Plast Ind 2002, 30, 17.
16. Duesberg, G. S.; Blau, W.; Byrne, H. J.; Master, J. Synth Met 1999, 103, 2484.
17. Hernadi, K.; Siska, A.; Thien-Nga, L.; Forró, L.; Kiricsi, I. Solid State Ion 2001, 141, 203.
18. Chen, G. X.; Kim, H. S.; Park, B. H.; Yoon, J. S. Polymer 2006, 47, 4760.
19. Kim, H. S.; Park, B. H.; Yoon, J. S.; Jin, H. J. Mater Lett 2007, 61, 2251.
20. Kang, M. S.; Myung, S. J.; Jin, H. J. Polymer 2006, 47, 3961.
21. Zeng, H. L.; Gao, C.; Wang, Y. P.; Watts, P. C. P.; Kong, H.; Cui, X. W.; Yan, D. Y. Polymer 2006, 47, 113.
22. Haggenmueller, R.; Du, F. M.; Fischer, J. E.; Winey, K. I. Polymer 2006, 47, 2381.
23. Li, J.; Tong, L. F.; Fang, Z. P.; Gu, A. J.; Xu, Z. B. Polym Degrad Stab 2006, 91, 2046.
24. Shao, W. G.; Wang, Q.; Wang, F.; Chen, Y. H. Carbon 2006, 44, 2708.
25. Zhao, C. G.; Hu, G. J.; Justice, R.; Schaefer, D. W.; Zhang, S. M.; Yang, M. S.; Charles, C.; Han, C. C. Polymer 2005, 46, 5125.
26. Jose, M. V.; Steinert, B. W.; Thomas, V.; Dean, D. R.; Abdalla, M. A.; Price, G.; Janowski, G. M. Polymer 2007, 48, 1096.
27. Sandler, J. K. W.; Pegel, S.; Cadek, M.; Gojny, F.; van Es, M.; Lohmar, J.; Blau, W. J.; Schulte, K.; Windle, A. H.; Shaffer, M. S. P. Polymer 2004, 45, 2001.
28. Li, J.; Fang, Z. P.; Tong, L. F.; Gu, A. J.; Liu, F. Eur Polym J 2006, 42, 3230.
29. Benedict, L. X.; Louie, S. G.; Cohen, M. L. Phys Rev B 1995, 52, 8541.
30. Berber, S.; Kwon, Y. K.; Tomanek, D. Phys Rev Lett 2000, 84, 4613.